Received: 5 November 2023 | Revised: 18 January 2024 | Accepted: 3 February 2024

DOI: 10.1111/mpp.13439

Molecular Plant Pathology WILEY

ORIGINAL ARTICLE

# MoAti1 mediates mitophagy by facilitating recruitment of MoAtg8 to promote invasive growth in *Magnaporthe oryzae*

**Huanbin Shi**[1] | **Shuai Meng**[1] | **Jiehua Qiu**[1] | **Shuwei Xie**[1] | **Nan Jiang**[1] | **Chaoxi Luo**[2] | **Naweed I. Naqvi**[3] | **Yanjun Kou**[1]

[1]State Key Lab of Rice Biology and Breeding, China National Rice Research Institute, Hangzhou, China

[2]Key Lab of Horticultural Plant Biology, Ministry of Education, and College of Plant Science and Technology, Huazhong Agricultural University, Wuhan, China

[3]Temasek Life Sciences Laboratory, Department of Biological Sciences, National University of Singapore, Singapore

**Correspondence**
Yanjun Kou, State Key Lab of Rice Biology and Breeding, China National Rice Research Institute, Hangzhou 311400, China.
Email: kouyanjun@caas.cn

**Funding information**
National Natural Science Foundation of China, Grant/Award Number: 32000103 and 32100161; National Key Research and Development Program of China, Grant/Award Number: 2022YFD1401500 and 2023YFD1400200; key RD project of China National Rice Research Institute, grand number, Grant/Award Number: CNRRI202004; Key Projects of Zhejiang Provincial Natural Science Foundation, Grant/Award Number: LZ23C130002 to JQ

## Abstract

Mitophagy is a selective autophagy for the degradation of damaged or excessive mitochondria to maintain intracellular homeostasis. In *Magnaporthe oryzae*, a filamentous ascomycetous fungus that causes rice blast, the most devastating disease of rice, mitophagy occurs in the invasive hyphae to promote infection. To date, only a few proteins are known to participate in mitophagy and the mechanisms of mitophagy are largely unknown in pathogenic fungi. Here, by a yeast two-hybrid screen with the core autophagy-related protein MoAtg8 as a bait, we obtained a MoAtg8 interactor MoAti1 (MoAtg8-interacting protein 1). Fluorescent observations and protease digestion analyses revealed that MoAti1 is primarily localized to the peripheral mitochondrial outer membrane and is responsible for recruiting MoAtg8 to mitochondria under mitophagy induction conditions. MoAti1 is specifically required for mitophagy, but not for macroautophagy and pexophagy. Infection assays suggested that MoAti1 is required for mitophagy in invasive hyphae during pathogenesis. Notably, no homologues of MoAti1 were found in rice and human protein databases, indicating that MoAti1 may be used as a potential target to control rice blast. By the host-induced gene silencing (HIGS) strategy, transgenic rice plants targeted to silencing *MoATI1* showed enhanced resistance against *M. oryzae* with unchanged agronomic traits. Our results suggest that *MoATI1* is required for mitophagy and pathogenicity in *M. oryzae* and can be used as a target for reducing rice blast.

**KEYWORDS**
Atg8, fungal pathogen, pathogenicity, rice blast, selective autophagy

## 1 | INTRODUCTION

Mitochondria, which are double-membrane-enclosed organelles, are responsible for the majority of the cellular oxidative processes and produce a large amount of cellular adenosine triphosphate (ATP) to provide energy for cells (Friedman & Nunnari, 2014). In addition to such energy supply for cells, mitochondria play vital roles in a range of processes such as cell division, cellular differentiation, cell signalling and cell death (Mehta et al., 2017; Zhong et al., 2016). However, stresses from the external environment or host result in

Huanbin Shi and Shuai Meng contributed equally to this work.

the formation of defective mitochondria, which are detrimental to cellular homeostasis. Effective mitochondrial quality and quantity control systems, including mitophagy, a selective autophagy, have evolved to restore and preserve cellular homeostasis (Ng et al., 2021; Palikaras et al., 2018).

Mitophagy is a kind of autophagic process that specifically targets and eliminates impaired or superfluous mitochondria to maintain cellular integrity and promote cellular renewal. Mitophagy can be induced by various stresses, including nitrogen starvation conditions, oxidative stress conditions and rapamycin treatment, as well as damage to mitochondrial functions (He et al., 2013; Nagi et al., 2016; Onishi et al., 2021; Youle & Narendra, 2011). When mitophagy is induced, the mitophagy receptors, proteins located on the outer mitochondrial membrane, recruit the core autophagic machinery, including the ubiquitin-like protein Atg8/LC3 (light chain-3), at the phagophore assembly sites (PAS). Many mitophagy receptors have been characterized, such as Atg32, in *Saccharomyces cerevisiae*, the NIX (Nip3-like protein X, BNIP3L), BNIP3 (BCL20 interacting protein 3), BCL2L13 (Bcl-2-like protein 13, Atg32 homologues), FUNDC1 (FUN14 domain-containing protein 1), PHB2 (prohibitin 2), FKBP8 (anti-apoptotic FK506-binding protein 8), OPTN (optineurin), MTP18 and ATAD3B (ATPase family AAA domain-containing 3B) in mammals, TraB in *Arabidopsis thaliana* and Atg43 in *Schizosaccharomyces pombe* (Bhujabal et al., 2017; Fukuda et al., 2020; Li, Duckney, et al., 2022; Liu et al., 2012; Meyer et al., 2023; Murakawa et al., 2015; Novak et al., 2010; Okamoto et al., 2009; Panigrahi et al., 2023; Quinsay et al., 2010; Shu et al., 2021; Wei et al., 2017).

Atg8/LC3 interacts with mitophagy receptors through the Atg8-family interacting motif (AIM in yeast)/LC3-interacting region (LIR in mammals), a conserved WXXL-like sequence (W/Y-X-X-L/I/V), which mediates the selective recognition of damaged or excessive mitochondria by the phagophore (Okamoto et al., 2009; Onishi et al., 2021; Palikaras et al., 2018; Xie et al., 2008; Youle & Narendra, 2011). Subsequently, an autophagosome completely encloses the mitochondrion to depolarize and degrade superfluous, damaged and dysfunctional mitochondria (Feng et al., 2014). Therefore, mitophagy is a core mechanism for conserving valuable nutrients from being consumed inefficiently and plays a key prevention role in the generation of reactive oxygen species, so as to maintain proper intracellular homeostasis, cell survival, growth and differentiation (Onishi et al., 2021; Palikaras et al., 2018; Youle & Narendra, 2011). Although mitophagy has been studied extensively in *S. cerevisiae* and mammalian cells (Palikaras et al., 2018; Youle & Narendra, 2011), only a few proteins that participate in mitophagy have been identified and the mechanisms of mitophagy remain largely unknown, especially in pathogenic fungi.

The filamentous ascomycetous fungus *Magnaporthe oryzae* causes rice blast, the most devastating disease of rice worldwide (Dean et al., 2012; Yan & Talbot, 2016). During the infection by *M. oryzae*, three-celled conidia are deposited by rain splashes and adhere to the surface of rice plants. Under suitable conditions, the conidia germinate and form appressoria to penetrate the rice cuticles. Once inside the host cells, *M. oryzae* differentiates into invasive hyphae and spreads to neighbouring cells to form typical lesions (Valent, 2021). Our recent study has shown that mitophagy occurs in *M. oryzae* during the transition from biotrophy to necrotrophy, and is required for the proper induction and establishment of rice blast disease (Kou et al., 2019). This process requires the sorting nexin Snx4/MoAtg24, which assists mitophagy in foot cells for conidiation and invasive hyphae for pathogenesis (He et al., 2013). In addition, the mitochondrial fission-related proteins, including MoDnm1, MoFis1 and MoMdv1, are also involved in the mitophagy and pathogenicity in *M. oryzae* (Khan et al., 2015; Zhong et al., 2016). Recently, an investigation revealed that MoMsn2 regulates the expression level of putative 3-methyglutaconyl-CoA hydratase-encoding gene to control mitophagy, which is important for the pathogenesis of *M. oryzae* (Xiao et al., 2021). However, the mechanism of mitophagy during pathogenesis requires further exploration in *M. oryzae*.

SUN (SIM1, UTH1, NCA3 and SUN4) family proteins share a high homology in their C-terminal domain, which is composed of 258 amino acids, and are involved in different cellular processes, such as DNA replication, lifespan, mitochondrial biogenesis and cell septation (Camougrand et al., 2000; Kissova et al., 2004; Mouassite, Camougrand, et al., 2000; Mouassite, Guérin, et al., 2000; Velours et al., 2002). In yeast, a SUN family protein Uth1 was initially identified based on its role in the regulation of longevity (Camougrand et al., 2000), and was later found to be involved in mitophagy (Camougrand et al., 2003; Kissova et al., 2004). In another report, the mitophagy rates of Δ*uth1* mutant under different induction conditions were compared with those of the wild type, demonstrating that mitophagy could be induced normally in cells lacking Uth1 in yeast (Welter et al., 2013). Currently, it remains unclear whether SUN family proteins participate in mitophagy.

In this study, we set out to identify the proteins potentially participating in mitophagy in *M. oryzae* by screening the interacting proteins of the core autophagy-related protein MoAtg8. We show that one of the MoAtg8-interacting proteins MoAti1, a SUN family protein, is specifically required for mitophagy by facilitating recruitment of MoAtg8 to mitochondria. MoAti1 mediates mitophagy in the invasive hyphae and contributes to the establishment of the blast disease in rice. Furthermore, the host-induced gene silencing (HIGS) of *MoATI1* enhanced resistance against blast in rice.

## 2 | RESULTS

### 2.1 | MoAti1 interacts with the core autophagy-related protein MoAtg8 in *M. oryzae*

MoAtg8, the only one homologue of mammalian LC3 or yeast Atg8 in *M. oryzae*, serves as a core autophagy-related protein required for autophagy (Veneault-Fourrey et al., 2006). When mitophagy is induced by specific physiological stresses, some mitochondrial proteins bind

to the Atg8/LC3 homologues on the forming autophagosomal membranes to allow membrane expansion along the surface of degraded mitochondria (Nakatogawa et al., 2007; Ng et al., 2021; Palikaras et al., 2018). To identify potential proteins participating in mitophagy and study their regulatory effect on cellular processes in *M. oryzae*, a yeast-two-hybrid (Y2H) screen was conducted using an *M. oryzae* cDNA library with MoAtg8 as the bait. Among 32 physically interacting candidates obtained from the Y2H screening (Table S1), we focused on *MGG_00505*, which encodes a predicted mitochondrial protein consisting of 416 amino acid residues. This protein was designated as MoAti1 (MoAtg8-interacting protein 1). Sequence analysis indicated that MoAti1 contains a conserved SUN domain (Figure S1). In addition, MoAti1 shares 39.21%, 37.77% and 35.94% amino acid sequence identity with yeast SUN family proteins Uth1, Sun4 and Nca3, respectively (Kissova et al., 2004).

To further validate the interaction between MoAtg8 and MoAti1, a DUAL membrane system analysis was performed with pBT3-SUC-MoAti1 and pPR3-N-MoAtg8. The results confirmed the interaction in yeast as detailed in Figure 1a. Furthermore, the results of a co-immunoprecipitation (Co-IP) analysis with the *MoATI1-mCherry/GFP-MoATG8* strain confirmed this interaction in vivo (Figure 1b). Then, glutathione S-transferase (GST)-tagged MoAtg8 and His-tagged MoAti1 were expressed in *Escherichia coli* BL21(DE3). A GST pull-down assay showed that GST-MoAtg8 interacted with His-Ati1

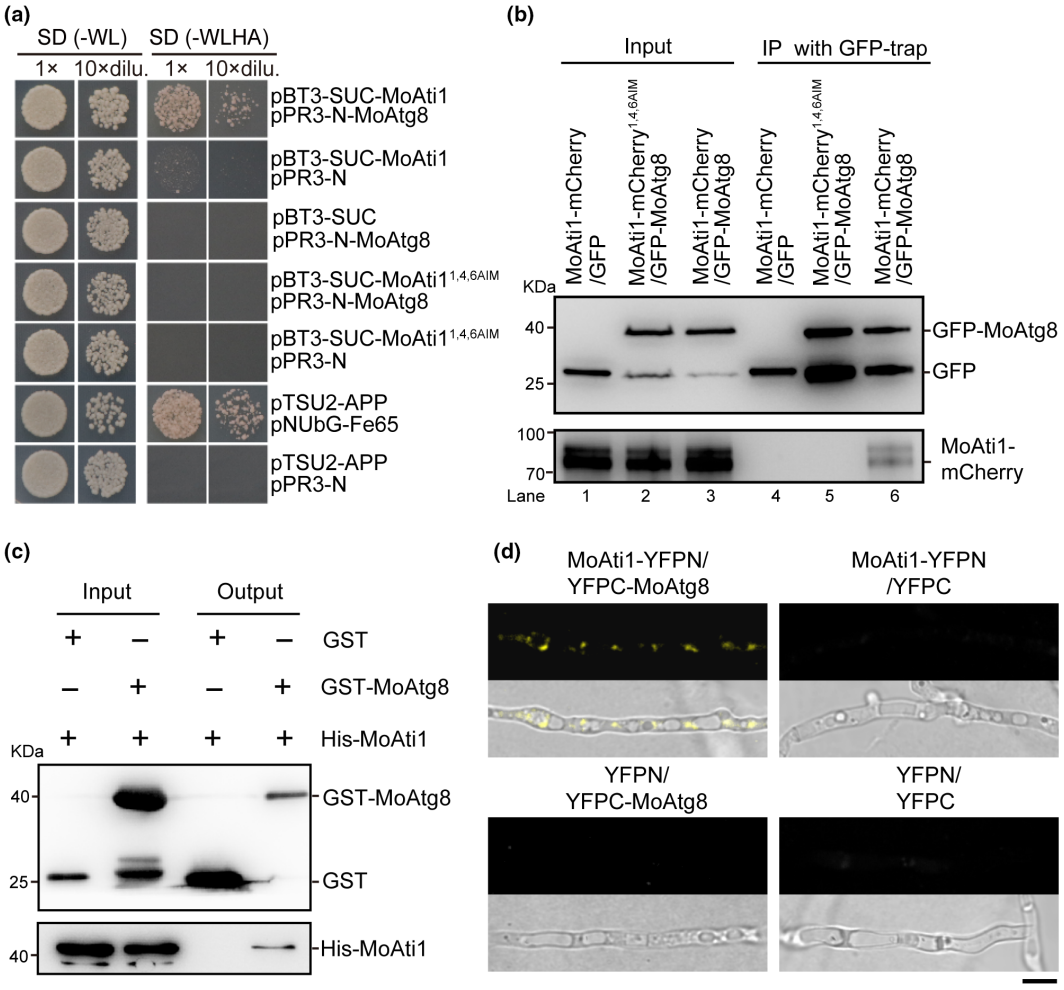


**FIGURE 1** MoAti1 interacts with the core autophagy-related protein MoAtg8. (a) DUAL membrane yeast two-hybrid assay for testing the interaction between MoAti1 and MoAtg8. Yeast transformants with the indicated plasmids were diluted and cultured on the SD−WL and SD−WLHA media for 4 days before imaging. The mutated protein MoAti1$^{1,4,6AIM}$, which was generated by mutating the first, fourth and sixth predicted AIM/LIR motifs in MoAti1, could not interact with MoAtg8. (b) Co-immunoprecipitation assay for testing the interaction between MoAti1 and MoAtg8 in *Magnaporthe oryzae*. The fusion protein MoAti1-mCherry (71 kDa) was co-precipitated with GFP-MoAtg8 (40 kDa). In contrast, the AIM/LIR-mutated MoAti1$^{1,4,6AIM}$ fusion protein failed to be detected in the eluted protein solution from the strain co-expressing GFP-MoAtg8 and MoAti1$^{1,4,6AIM}$-mCherry. Free GFP (27 kDa) in lanes 2 and 3 is caused by basal autophagy. The *MoATI1-mCherry/GFP* strain served as a negative control. (c) Pull-down assay for determining the interaction between MoAti1 and MoAtg8. The fusion protein His-Ati1 was detected in the eluted solution of GST-MoAtg8 and His-MoAti1 co-incubated mixture, but not in that of glutathione S-transferase (GST) and His-MoAti1. (d) Bimolecular fluorescence complementation assay for examining the interaction between MoAti1 and MoAtg8. Yellow fluorescent protein (YFP) fluorescence is observed in mycelia co-expressing MoUth1-YFPN and YFPC-MoAtg8. Bar = 5 μm. Consistent results were obtained from two biological replicates.

(Figure 1c). The interaction between MoAti1 and MoAtg8 was further confirmed by a bimolecular fluorescence complementation (BiFC) assay. Dotted yellow fluorescent protein (YFP) fluorescence was seen in the mycelia co-expressing MoAti1-YFP and YFPC-MoAtg8 (Figure 1d). Some Atg8-binding proteins interact with Atg8/LC3 through AIM/LIR motifs (Fracchiolla et al., 2017; Palikaras et al., 2018). To determine whether MoAti1 has potential AIM/LIR motifs, the protein sequence of MoAti1 was analysed using the iLIR database, and six potential AIM/LIR motifs were identified (Figure S2a) (Jacomin et al., 2016). Then, to determine which motifs were functional in binding with MoAtg8, point mutations of the AIM/LIR motifs in MoAti1 were generated and cloned into pBT3-SUC to perform the DUALmembrane system analysis. The results revealed that the interaction between MoAti1 and MoAtg8 was weakened by the mutations in the first, fourth and sixth AIM/LIR motifs (Figures 1a and S2b). Consistent with the results of the Y2H analysis, the Co-IP data also showed that simultaneous mutations in the first, fourth and sixth motifs abolished the interaction between MoAti1 and MoAtg8 in *M. oryzae* (Figure 1b). These results suggested that all of the first, fourth and sixth AIM/LIR motifs in MoAti1 are required for the physical interaction with MoAtg8.

## 2.2 | MoAti1 is partly located in the peripheral mitochondrial outer membrane

To investigate the biological roles of MoAti1 in *M. oryzae*, we first determined its subcellular localization. The C terminus of MoAti1 tagged with mCherry, which did not affect the function of MoAti1, was introduced into the *M. oryzae* Mito-GFP strain. This strain expresses a subunit of F1 sector of mitochondrial F1F0 ATP synthase (Atp1)-GFP fusion protein, a widely used mitochondrial marker (He et al., 2013; Kou et al., 2019; Patkar et al., 2012). Fluorescent observation with a confocal microscope showed that the fluorescent signal of MoAti1-mCherry primarily presented on the punctate and tubular structures, overlapping with the mitochondrial marker Mito-GFP in the conidia and hyphae under normal growth conditions (Figure 2a).

Next, the mitochondrial localization of MoAti1 was further examined using a biochemical approach. Mitochondrial proteins were fractionated from the total proteins of the strain expressing both MoAti1-GFP and MoTim23-mCherry, a mitochondrial integral membrane protein (Figure 2b) (Zhou et al., 2008). The immunoblotting results revealed that the majority of MoAti1 was enriched in the mitochondrial fraction, with a small amount in the cytoplasm (Figure 2c). In contrast, the cytoplasmic protein glyceraldehyde-3-phosphate dehydrogenase (GAPDH) was only enriched in the cytoplasmic fraction (Figure 2c). In *M. oryzae*, MoAti1 does not have transmembrane domains by the prediction using TMHMM-2.0. To determine how MoAti1 is located in the mitochondrial membrane, mitochondria were isolated from a strain expressing MoAti1-GFP and MoTim23-mCherry. The isolated mitochondria were then subjected to sodium carbonate treatment, a method commonly used to distinguish integral membrane proteins from peripheral membrane proteins (Kim et al., 2015). Immunoblotting analysis of the extracted mitochondrial proteins revealed that MoAti1 was only detected in the supernatant, while integral mitochondrial membrane proteins, such as MoTim23-mCherry and Porin, were present in the pellet fraction (Figure 2d). These observations suggested that MoAti1 is a peripheral mitochondrial membrane protein.

To further distinguish if the localization of MoAti1 is on the outer mitochondrial membrane, inner boundary membrane or mitochondrial matrix, isolated mitochondria from a strain co-expressing MoAti1-GFP and MoCox11-mCherry, an inner mitochondrial membrane marker protein, were used to refine the submitochondrial localization of MoAti1 using a protease digestion assay with different concentrations of proteinase K (Besingi & Clark, 2015). The proteolysis pattern of MoAti1 was similar to that of the outer mitochondrial membrane protein Porin, but not to the mitochondrial inner membrane protein MoCox11 or the mitochondrial matrix protein MoHsp60 (Figure 2e,f), indicating that the majority of MoAti1 is located peripherally at the outer mitochondrial membrane.

## 2.3 | MoAti1 is required for mitophagy

The interaction between MoAti1 and MoAtg8, as well as the localization of MoAti1 to mitochondria, suggested that MoAti1 may play a role in mitophagy. To investigate whether MoAti1 is involved in mitophagy, the fluorescent dynamics of MoAti1-mCherry were observed under nutrient-rich or nitrogen-starvation conditions. After being subjected to nitrogen starvation for 12 h, Mito-GFP and MoAti1-mCherry were found to accumulate in the vacuoles, which were visualized by 7-amino-4-chloromethylcoumarin (CMAC) staining in *M. oryzae*, indicating that the MoAti1-mCherry is targeted to the vacuoles along with mitochondria upon nitrogen starvation (Figure S3a). In contrast, the deletion of *MoATG8* inhibited the targeting of MoAti1-mCherry to the vacuoles under nitrogen-starvation conditions, indicating that this process was probably dependent on the MoAtg8-mediated autophagy (Figure S3b). These results indicated that MoAti1 is imported into vacuoles along with mitochondria upon nitrogen starvation in *M. oryzae*.

In order to observe the effects of loss of *MoATI1* on mitochondrial behaviour and function, the Δ*Moati1/Mito-GFP* strain was generated in the Mito-GFP background using a standard one-step gene replacement strategy. Subsequently, complementation analysis was performed (Figure S4). In the Mito-GFP strain, when mitophagy was induced, a portion of the Mito-GFP protein was delivered into vacuoles for degradation (He et al., 2013; Kou et al., 2019). Compared to the evident mitochondrial GFP signals in the vacuoles of the Mito-GFP strain, much less GFP signal was observed in the CMAC-stained vacuoles of the Δ*Moati1/Mito-GFP* strain upon nitrogen starvation (Figure 3a), implicating a role for MoAti1 in mitophagy. More stable Mito-GFP could be detected by immunoblot analysis in the Δ*Moati1/Mito-GFP* strain than in the *Mito-GFP* strain upon nitrogen starvation (Figure 3b). The mitophagy was monitored by assessing the total amount of Porin as a

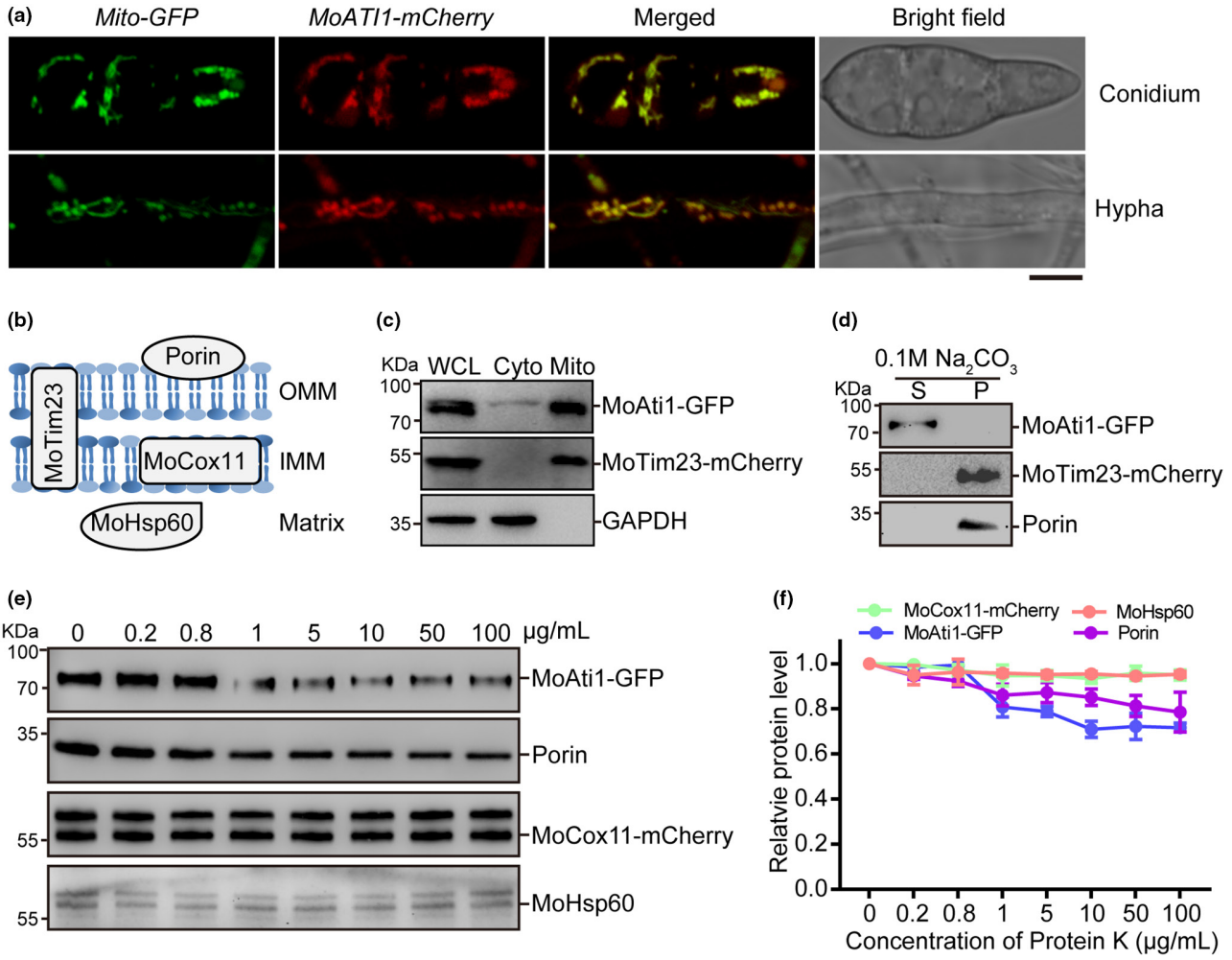


**FIGURE 2** MoAti1 is an outer mitochondrial membrane protein. (a) Fluorescent co-localization of MoAti1-mCherry and mitochondria marker Mito-GFP in conidia and hyphae of *Magnaporthe oryzae*. Bar = 5 μm. (b) Schematic presentation of submitochondrial protein markers used in this study. OMM, outer mitochondrial membrane; IMM, inner mitochondrial membrane. (c) MoAti1 is predominantly detected in the mitochondrial fraction. Cytoplasmic proteins (Cyto) and mitochondrial proteins (Mito) isolated from strains expressing MoAti1-GFP (71 kDa) and MoTim23-mCherry (53 kDa) were analysed with immunoblotting using antibodies against green fluorescent protein (GFP), mCherry and glyceraldehyde-3 phosphate dehydrogenase (GAPDH). WCL, whole cell lysate. (d) MoAti1 exhibits peripheral localization on the mitochondria. The isolated mitochondrial proteins were treated with sodium carbonate solution. The resultant pellet (P) and supernatant (S) were subjected to immunoblotting using antibodies against GFP, mCherry and Porin. (e) The isolated mitochondria from strains expressing MoAti1-GFP and MoCox11-mCherry (56 kDa) were treated with a range of concentrations of proteinase K followed by immunoblotting analysis. The proteolysis of MoAti1-GFP by proteinase K was similar to that of the outer mitochondrial membrane protein Porin (32 kDa). MoHsp60, 60 kDa. (f) Relative protein levels of the indicated proteins in (e) were measured using ImageJ software. Data are presented as mean ± *SD*. The immunoblotting analysis was performed with two biological replicates, and consistent results were obtained in both cases.

mitochondrial marker protein (He et al., 2013; Zhong et al., 2016). In contrast to the *Mito-GFP* strain, the Porin degradation was not obvious in the Δ*Moati1*/*Mito-GFP* mutant upon nitrogen starvation for 12 h (Figure 3b). All these results indicated that MoAti1 is necessary for mitophagy.

## 2.4 | MoAti1 recruits MoAtg8 to mitochondria through the AIM/LIR motifs

To gain further insights into the involvement of MoAti1 in mitophagy, we initially focused on closely monitoring the co-localization of MoAti1 with the core autophagy-related protein MoAtg8 during the process of mitophagy. The *MoATI1-mCherry* was constructed and transformed into the *GFP-MoATG8* strain. As shown in Figure 4a, the co-localization of the fluorescence signals of the MoAti1-mCherry and GFP-MoAtg8 were observed in the *MoATI1-mCherry*/*GFP-MoATG8*/Δ*Moati1* strain. Due to crucial roles of the AIM/LIR motifs in the interaction between MoAti1 and MoAtg8, we then determined whether the AIM/LIR motifs are required for the co-localization of MoAti1-mCherry and GFP-MoAtg8. The mutated *MoATI1*$^{1,4,6AIM}$-*mCherry* and *GFP-MoATG8* were sequentially transformed into the Δ*Moati1* strain. The results revealed that the red and green fluorescent signals of the MoAti1$^{1,4,6AIM}$-mCherry and the GFP-MoAtg8

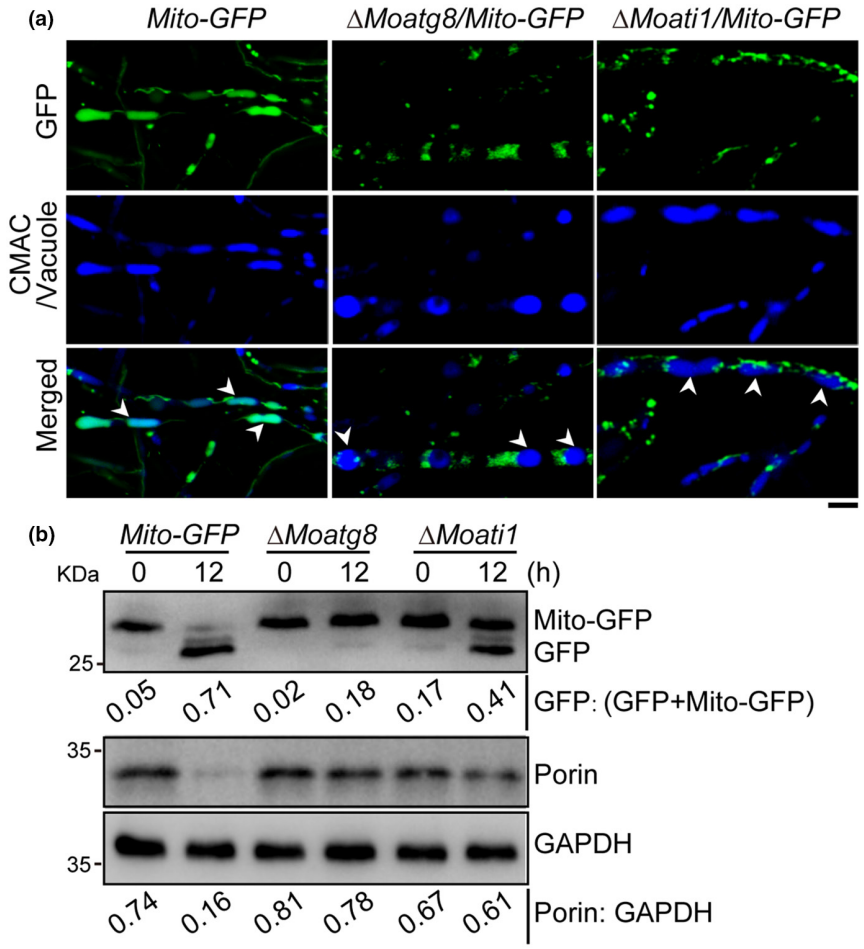


**FIGURE 3** MoAti1 is required for mitophagy in *Magnaporthe oryzae*. (a) Fluorescent observations revealed the impaired mitophagy in the Δ*Moati1* mutant. Fluorescent microscopy observations of the green fluorescent protein (GFP) signals in the *Mito-GFP*, Δ*Moatg8/Mito-GFP* and Δ*Moati1/Mito-GFP* strains upon nitrogen starvation for 6 h. Similar to the Δ*Moatg8/Mito-GFP* strain, the Mito-GFP could not be delivered into 7-amino-4-chloromethylcoumarin (CMAC)-stained vacuoles for degradation in the Δ*Moati1* mutant, whereas the GFP signals overlapped with vacuoles in the *Mito-GFP* strain. Arrows indicate the vacuoles where Mito-GFP enters or not in the indicated strains. (b) Mitophagy defects in the Δ*Moati1/Mito-GFP* strains were demonstrated via immunoblot analysis. The mycelia of the *Mito-GFP* strain and the mutant were cultured in a complete medium for 2 days and then transferred to a glycerol medium for 30 h followed by nitrogen starvation for 12 h. The total proteins extracted from the aforementioned mycelia were subjected to immunoblot analysis using anti-GFP or anti-Porin antibodies. The mitophagy levels were assessed by calculating the ratios of free GFP to total GFP or the ratios of Porin to glyceraldehyde-3-phosphate dehydrogenase (GAPDH). The degree of degradation of the mitochondrial markers Mito-GFP and Porin was reduced in the Δ*Moati1/Mito-GFP* mutants compared with those of the *Mito-GFP* strain. Consistent results were obtained from three replicates.

failed to overlap under both normal growth and nitrogen-starvation conditions (Figure 4a), suggesting that the first, fourth and sixth AIM/LIR motifs are required for the co-localization of MoAti1 and MoAtg8. In addition, the mutated *MoATI1*$^{1,4,6AIM}$*-mCherry* still located in mitochondria but could not rescue the mitophagy defects of the Δ*Moati1* mutant (Figures S5 and S6), indicating that the co-localization and interaction between MoAti1 and MoAtg8 are important for the MoAti1-mediated mitophagy.

These results led to a hypothesis in which MoAti1 might function by recruiting MoAtg8 to mitochondria under mitophagy induction conditions. To test this, the *mCherry-MoATG8/Mito-GFP*, Δ*Moati1/mCherry-MoATG8/Mito-GFP* and *MoATI1*$^{1,4,6AIM}$/Δ*Moati1/mCherry-MoATG8/Mito-GFP* strains were generated to observe the recruitment of MoAtg8 to mitochondria when *MoATI1* is deleted or mutated. As shown in Figure 4c, the mCherry-MoAtg8 was diffusely distributed in the cytoplasm in the *mCherry-MoATG8/Mito-GFP* strain under normal growth conditions. However, upon nitrogen starvation, the co-localization of the mCherry-MoAtg8 and Mito-GFP was observed in the *mCherry-MoATG8/Mito-GFP* strain (Figure 4b,c). In contrast, the co-localization of the mCherry-MoAtg8 and Mito-GFP was rarely observed in the Δ*Moati1/mCherry-MoATG8/Mito-GFP* and *MoATI1*$^{1,4,6AIM}$/Δ*Moati1/mCherry-MoATG8/Mito-GFP* strains (Figure 4b,c). The Mito-GFP failed to be delivered into the CMAC-labelled vacuoles for degradation in both Δ*Moati1/mCherry-MoATG8/Mito-GFP* and *MoATI1*$^{1,4,6AIM}$/Δ*Moati1/mCherry-MoATG8/Mito-GFP* strains (Figure 4b). The mCherry-MoAtg8 could be successfully imported into the vacuoles due to functional macroautophagy in all these strains (Figure 4b,c). Immunoblotting analysis

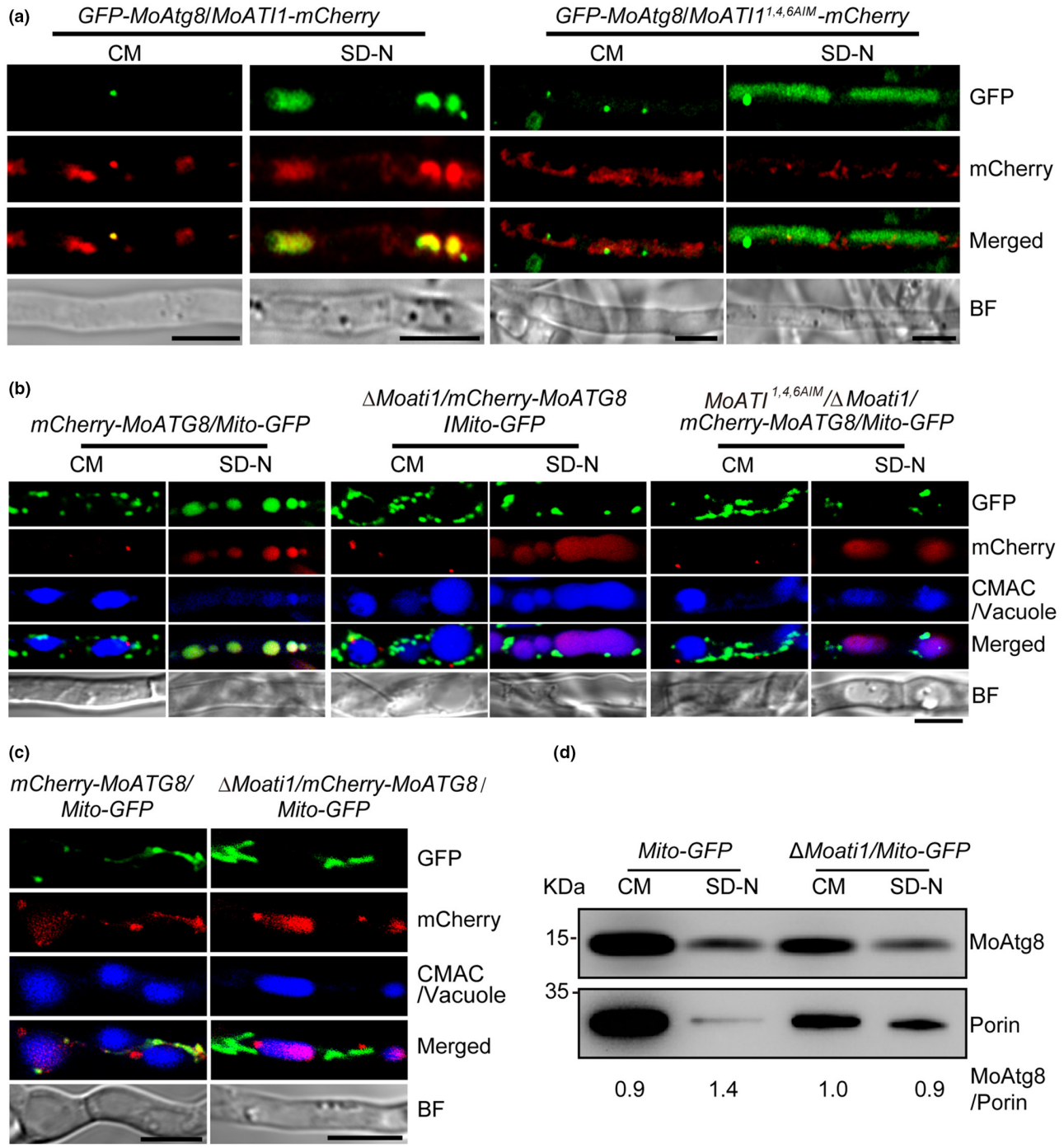


**FIGURE 4** MoAti1 recruits MoAtg8 to mitochondria via the AIM/LIR motifs. (a) AIM/LIR motifs are required for the co-localization of MoAti1 and MoAtg8. The MoAti1-mCherry co-localized with the GFP-MoAtg8 on the autophagosomes (dotted fluorescence) in the hyphae. Mutations of the first, fourth and sixth AIM motifs led to the failure in co-localization of the MoAti1-mCherry and the GFP-MoAtg8 in *Magnaporthe oryzae*. (b) Deletion of the *MoATI1* and the mutations of AIM/LIR motifs affected the recruitment of MoAtg8 to mitochondria during nitrogen starvation. Under nitrogen-starvation conditions, co-localization of the mCherry-MoAtg8 and the Mito-GFP was observed in the *mCherry-MoATG8/Mito-GFP* strain. However, this co-localization was disrupted in the Δ*Moati1/mCherry-MoATG8/Mito-GFP* and *MoATI1*$^{1,4,6AIM}$/Δ*Moati1/mCherry-MoATG8/Mito-GFP* strains. (c) The mCherry-MoAtg8 and the Mito-GFP were co-localized in the SD−N medium for 4 h. The vacuoles were stained with 7-amino-4-chloromethylcoumarin (CMAC). BF, bright field. Bar = 5 μm. (d) Deletion of *MoATI1* reduced MoAtg8 amount on mitochondria upon nitrogen starvation. Mitochondria were isolated from mycelia of the *Mito-GFP* and Δ*Moati1/Mito-GFP* cultured in complete medium (CM) and SD−N medium. The protein amounts of MoAtg8 (15 kDa) and Porin on mitochondria were detected with immunoblotting analysis. This experiment was performed with two biological replicates, and consistent results were obtained.

of mitochondrial extracts from the *Mito-GFP* and Δ*Moati1/Mito-GFP* strains revealed that disruption of *MoATI1* decreased the amount of MoAtg8 on mitochondria under conditions of mitophagy induction by nitrogen starvation (Figure 4d). Taken together, these results indicated that the deletion of *MoATI1* or mutation of the AIM/LIR motifs in *MoATI1* could significantly reduce the recruitment of MoAtg8 to mitochondria, consequently impairing mitophagy.

## 2.5 | MoAti1 is not necessary for macroautophagy and pexophagy

Proteins interacting with Atg8/LC3 may also be involved in macroautophagy and pexophagy (Liu et al., 2021). To ascertain whether MoAti1 is specifically required for mitophagy, deletion mutants of *MoATI1* were generated in the *GFP-MoATG8* strain, in which GFP-MoAtg8 serves a marker of macroautophagy (Klionsky et al., 2021). Under the macroautophagy inductive conditions, the co-localization of GFP-MoAtg8 with vacuoles was observed as previously reported (Li et al., 2021), and the degradation of GFP-MoAtg8 was detected via immunoblotting. The results showed that the macroautophagy levels in the Δ*Moati1/GFP-MoATG8* strain were comparable to that of the *GFP-MoATG8* stain under nitrogen-starvation conditions (Figure 5a,b). In addition, the pexophagy level in the Δ*Moati1/GFP-SRL* strain was similar to that of the *GFP-SRL* strain by observing the degradation of the GFP-labelled pexosomal signal protein GFP-SRL (Figure 5c). MoPex14 is a peroxisomal membrane protein that is essential for pexophagy in *M. oryzae* (Deng et al., 2013; Zutphen et al., 2008). Consistent with the microscopic observation, the degradation rate of the pexophagy marker protein MoPex14-GFP was not significantly different among the *MoPEX14-GFP* and Δ*Moati1/MoPEX14-GFP* strains (Figure 5d). Collectively, all the data indicated that MoAti1 is not necessary for macroautophagy and pexophagy but may be specifically required for mitophagy.

## 2.6 | MoAti1 is required for mitophagy in the invasive hyphae and establishment of rice blast disease

The expression of *MoATI1* is induced during the infection of *M. oryzae* (Figure 6a), indicating that *MoATI1* may play an important role in invasive growth. To investigate the biological roles

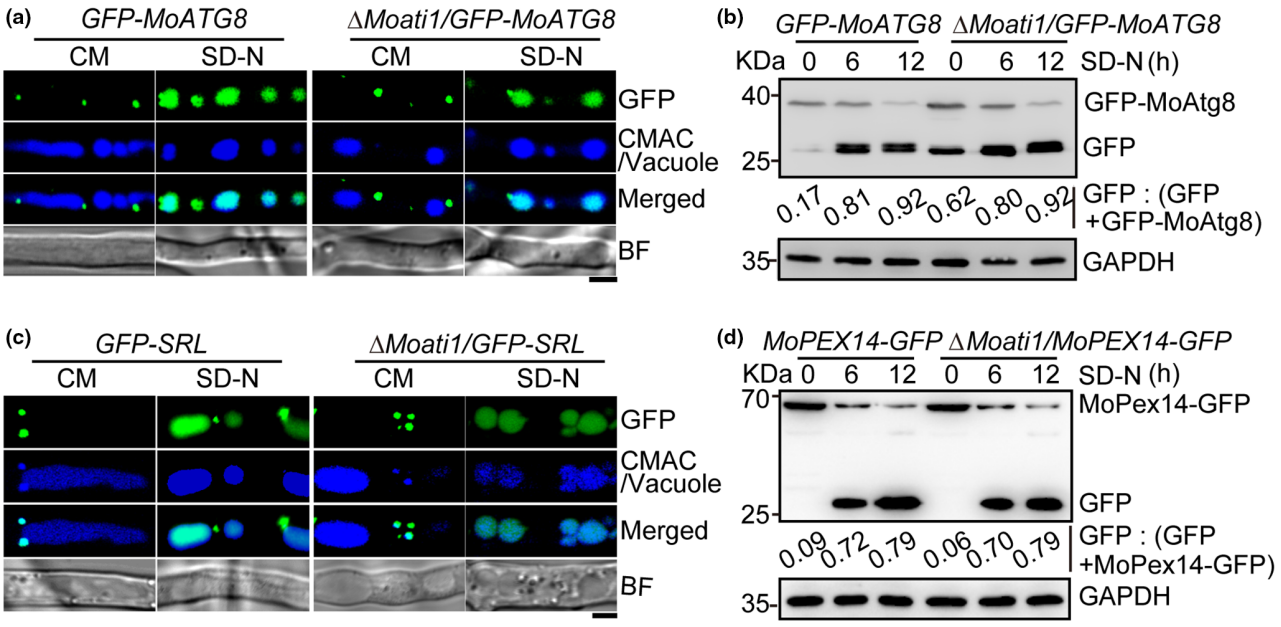


**FIGURE 5** MoAti1 is not necessary for macroautophagy and pexophagy in *Magnaporthe oryzae*. (a) Green fluorescent protein (GFP) fluorescent dynamics to monitor macroautophagy in the *GFP-MoATG8* and Δ*Moati1/GFP-MoATG8* strains. Mycelia of the *GFP-MoATG8* and Δ*Moati1/GFP-MoATG8* cultured in complete medium (CM) were transformed into SD−N medium for 12 h and then photographed. Under nitrogen-starvation conditions, GFP signals were observed in 7-amino-4-chloromethylcoumarin (CMAC)-stained vacuole in all strains, suggesting that macroautophagy occurs in the Δ*Moati1* mutant. (b) Degradation of the GFP-MoAtg8 fusion protein was detected by immunoblotting using an anti-GFP antibody. The fusion protein GFP-MoAtg8 was degraded normally in the Δ*Moati1/GFP-MoATG8* as the *GFP-MoATG8* strain in the SD−N medium. The numbers underneath the blots are the ratios of free GFP to total GFP to indicate the level of autophagy. Similar results were obtained from three replicates. (c) MoAti1 is not essential for pexophagy. Upon nitrogen starvation, the GFP-SRL indicated peroxisomes overlapped with CMAC-stained vacuoles in the Δ*Moati1/GFP-SRL* as the *GFP-SRL* strain. (d) Vacuolar degradation of the peroxisomes was detected by immunoblotting of MoPex14-GFP. The strains B157 and Δ*Moati1* expressing *MoPEX14-GFP* were cultured in CM for 2 days and then transferred to SD−N medium to induce pexophagy. The degradation dynamics of the fusion protein MoPex14-GFP were similar in the *MoPEX14-GFP* and Δ*Moati1/MoPEX14-GFP* strains. BF, bright field. Bar =2 μm.

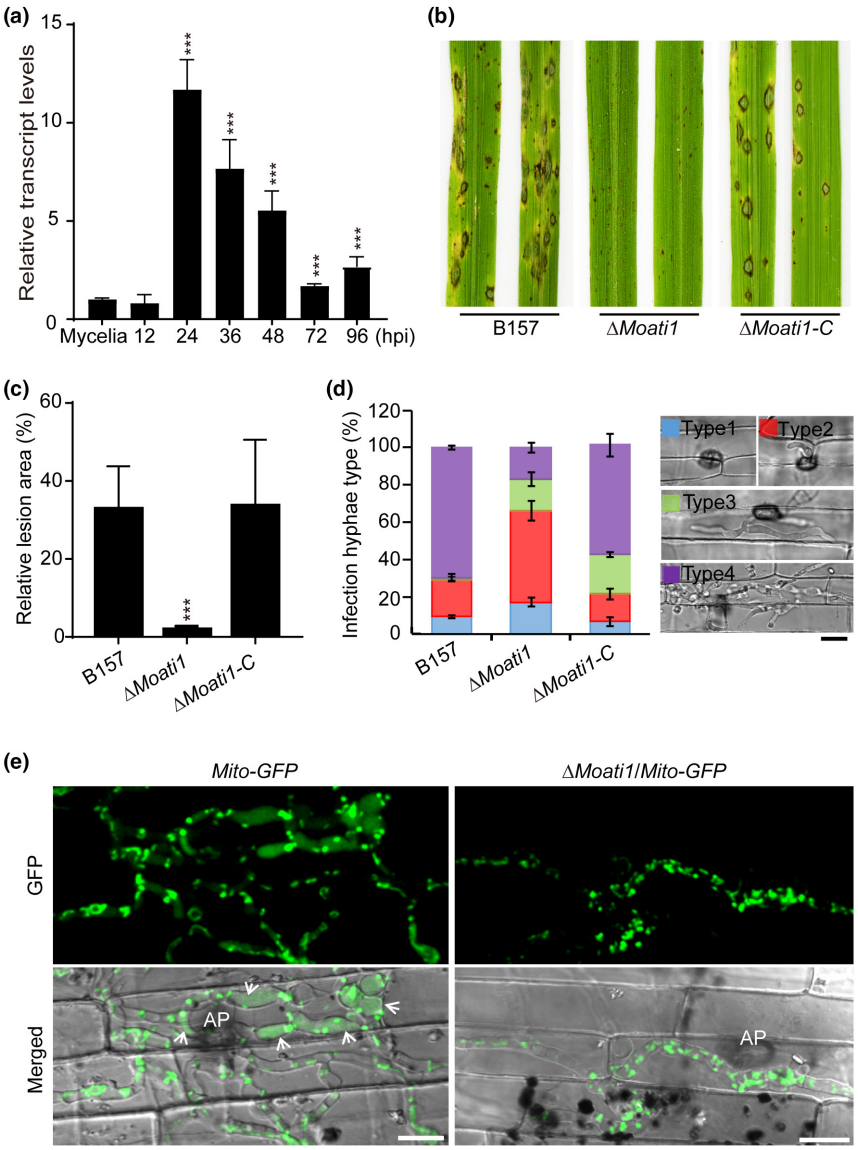


**FIGURE 6** *MoATI1* is required for mitophagy during invasive growth and pathogenicity. (a) Expression of *MoATI1* in *Magnaporthe oryzae* was highly induced during the invasive growth stage. hpi, hours post-inoculation. Data are shown as mean ± *SD* ($n = 3$). Asterisks represent significant differences with Student's *t* test at $p < 0.001$. (b) Disruption of *MoATI1* resulted in reduced virulence. Susceptible rice seedlings (*Oryza sativa* 'CO39') were inoculated with conidial suspensions of the wild-type strain B157 of *M. oryzae*, Δ*Moati1*, as well as complemented strains Δ*Moati1*-C. Images were taken at 7 dpi. (c) The bar chart shows the relative lesion areas calculated by ImageJ. Data are shown as mean ± *SD* ($n = 5$). Asterisks represent significant differences indicated by Student's *t* test at $p < 0.001$. (d) Deletion of *MoATI1* resulted in defects in spreading of invasive hyphae. Conidial drops of indicated strains were inoculated on the rice sheaths for 40 h to observe the invasive growth. Four types of appressoria were quantified (1, no penetration; 2, penetration with primary hyphae; 3, secondary invasive hyphae limited in the penetrated rice cell; 4, invasive hyphae spread to neighbouring cells). More than 200 appressoria from each indicated strain were counted each time. Bar = 10 μm. (e) The mitophagy process was impaired in the invasive hyphae of the Δ*Moati1/Mito-GFP* strain. Fluorescent observation of the GFP in the *Mito-GFP* and Δ*Moati1/Mito-GFP* strains during the invasive growth stage. Conidial suspensions of the indicated strains were inoculated on the rice sheaths of 3-week-old CO39 seedlings. Photographs were taken using a confocal microscope at 60 h post-inoculation. Arrows indicate vacuoles in the invasive hyphae. AP, appressorium.

of *MoATI1* in *M. oryzae*, the vegetative growth and pathogenicity were assayed by comparing the *Mito-GFP*, the Δ*Moati1/Mito-GFP* mutant and the complementation strain Δ*Moati1*-C/*Mito-GFP*. The Δ*Moati1/Mito-GFP* strain had smaller colonies when compared with the *Mito-GFP* and Δ*Moati1*-C/*Mito-GFP* strains on prune agar (PA) plates after 7 days' incubation (Figure S4d). To examine the role of MoAti1 on fungal pathogenicity, the conidia of the *Mito-GFP*, Δ*Moati1/Mito-GFP* and Δ*Moati1*-C/*Mito-GFP* strains were inoculated onto 21-day-old rice seedlings (*Oryza sativa* 'CO39'). The results revealed that, unlike the *Mito-GFP* and Δ*Moati1*-C/*Mito-GFP* strains that produced typical spindle-shaped blast lesions, the Δ*Moati1/Mito-GFP* mutant formed

smaller and restricted lesions (Figure 6b,c). To investigate the reason for the attenuation of virulence in the Δ*Moati1/Mito-GFP* mutant, a rice sheath infection assay was carried out. By assessment of the host penetration and invasive growth, we found that the appressoria from the Δ*Moati1/Mito-GFP* successfully penetrated rice sheathes but were compromised in developing proper invasive hyphae (Figure 6d). These results indicated that the highly reduced pathogenicity observed in the Δ*Moati1/Mito-GFP* strain is due to the impaired spreading of invasive hyphae from the host entry/invasion sites.

In our previous study, mitophagy was one of the important intermediate events between nutrient sensing and homeostasis in *M. oryzae*, leading to the establishment and extent of blast disease in rice plants (Kou et al., 2019). To further determine whether MoAti1-mediated mitophagy is required for pathogenicity in *M. oryzae*, the mitophagy in the invasive hyphae was examined in the Δ*Moati1/Mito-GFP* strains. As shown in Figure 6e, the fluorescent signals of Mito-GFP were clearly present in the vacuoles of the *Mito-GFP* invasive hyphae in the first invaded rice cell. In contrast, no obvious GFP signals were observed in the vacuoles of the Δ*Moati1/Mito-GFP* mutant, suggesting that the disruption of *MoATI1* interrupts mitophagy in the invasive hyphae in *M. oryzae*. Taken together, all these results suggested that MoAti1 is required for mitophagy in the invasive hyphae and contributes to the establishment of blast disease in rice.

### 2.7 | Host-induced gene silencing of MoATI1 enhances resistance to rice blast

In recent years, the application of host-induced gene silencing (HIGS) targeting fungal-specific pathogenicity genes has emerged as an effective strategy for controlling fungal diseases (Chen et al., 2022; Dou et al., 2020; Wang & Dean, 2022). This approach involves the generation of small interfering RNAs (siRNAs) by transgenic host plants that subsequently silence fungal-specific genes during infection (Cai et al., 2018). In this study, BLASTp analyses using the MoAti1 protein sequence as a query and BLASTn analyses using the *MoATI1* nucleotide sequence showed that no hits were identified in the protein and genome databases of rice and human (Table S2). MoAti1 is necessary for the pathogenicity of *M. oryzae*, so we hypothesized that it may be used as a potential target for controlling rice blast. To investigate whether HIGS targeting *MoATI1* could enhance host resistance to blast, *MoATI1* RNAi transgenic plants were generated in the rice line TP309, which is susceptible to blast. PCR and reverse transcription-quantitative PCR (RT-qPCR) verification confirmed the integration and expression of the RNAi cassette in two independent transgenic plants *MoATI1*-RNAi-4 and -6 (Figure S7). After being inoculated with conidial suspensions of *M. oryzae*, the wild-type seedlings developed numerous typical lesions, while the transgenic plants *MoATI1*-RNAi-4 and -6 exhibited fewer lesions and a lower amount of fungal biomass (Figure 7a–c). During the infection of the transgenic lines *MoATI1*-RNAi-4 and -6, the relative expression level of *MoATI1* in *M. oryzae* was lower compared to the wild-type TP309 (Figure 7d). Further rice sheath infection assay showed that at 36 h post-inoculation (hpi), more than 70% of infection hyphae spread to adjacent cells in the wild-type plants. In contrast, in *MoATI1*-RNAi plants, only about 30% of infection hyphae spread into adjacent cells (Figure 7e). Importantly, there were no significant differences in agronomic traits, including number of panicles, grain number per panicle, 1000-seed weight, plant height, grain length and grain width, between the transgenic plants (*MoATI1*RNAi-4 and -6) and their wild-type TP309 (Figures 7f–h and S8). In conclusion, all data indicated that HIGS of *MoATI1* conferred effective resistance to blast without changing agronomic traits in rice.

## 3 | DISCUSSION

In recent years, research in mitophagy has advanced rapidly, especially with the identification of some key receptors and regulatory factors (Liu et al., 2014; Meyer et al., 2023; Wei et al., 2017). However, the mitophagy in plant-pathogenic fungi has not yet been studied in detail. In this study, the fungal-specific pathogenicity gene *MoATI1* was characterized. The results of cell biology and biochemical analyses demonstrated that MoAti1 specifically participates in mitophagy by recruiting MoAtg8 to mitochondria through AIM/LIR motifs, and MoAti1-mediated mitophagy is required for pathogenesis in *M. oryzae*. Silencing *MoATI1* by a HIGS strategy confers resistance to *M. oryzae*. Our results offer novel insights into the molecular mechanism underlying mitophagy in filamentous fungi and obtain a good target for HIGS to develop blast-resistant rice plants.

In yeast, the role of SUN family proteins in mitophagy remains disputed. It was initially found that Uth1, a SUN family protein, is required for the responses to rapamycin under respiratory conditions with lactate as the sole carbon source, implying its involvement in mitophagy (Camougrand et al., 2003; Kissova et al., 2004). However, another research team has demonstrated that Uth1 is dispensable for mitophagy (Welter et al., 2013). In this study, it was found that there is only one SUN family protein homologue MoAti1 in *M. oryzae*, in contrast to the existence of four SUN family proteins in *S. cerevisiae* (Figure S1). Further evidence supports the hypothesis that MoAti1 is involved in mitophagy and potentially functions as a receptor of mitophagy in *M. oryzae*. First, MoAti1 is located in the outer membrane of mitochondria (Figure 2). Secondly, MoAti1 interacts with MoAtg8 through AIM/LIR motifs both in vitro and in vivo. MoAti1 is specifically required for mitophagy by facilitating the recruitment of MoAtg8 to mitochondria, while it is not essential for non-selective autophagy and pexophagy. Moreover, MoAti1 is necessary for mitophagy in nitrogen-starved mycelia and invasive hyphae in *M. oryzae*. All these characteristics align with those of the previously identified mitophagy receptors (Bhujabal et al., 2017; Fukuda et al., 2020; Li, Duckney, et al., 2022; Liu et al., 2012; Meyer et al., 2023; Murakawa et al., 2015; Novak et al., 2010; Okamoto et al., 2009; Panigrahi

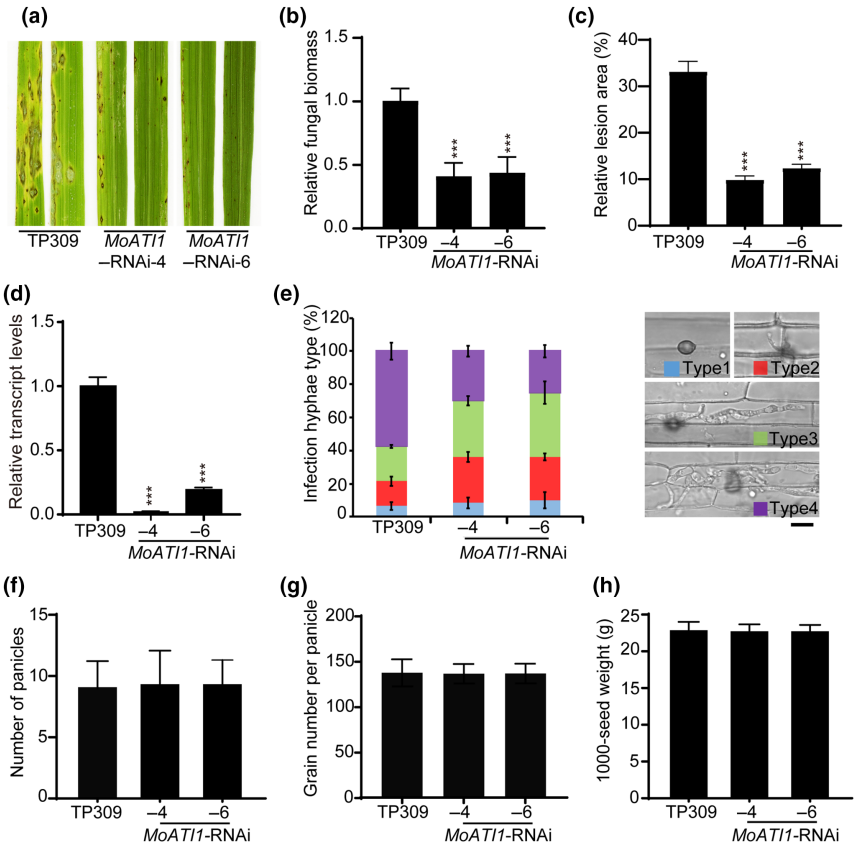


**FIGURE 7** Host-induced gene silencing of *MoATI1* strengthened blast resistance without changing agronomic traits in rice. (a) *Oryza sativa MoATI1-RNAi* lines exhibited elevated blast resistance. Smaller lesions developed on the leaves of *MoATI1-RNAi* lines inoculated with *Magnaporthe oryzae* B157 compared with those of the wild-type TP309. Relative fungal biomass (b) and relative lesion area (c) of the representative leaves of the wild-type TP309 and *MoATI1-RNAi* lines after inoculation with *M. oryzae*. (d) The relative transcript level of *MoATI1* in *M. oryzae* was lower in the *MoATI1-RNAi* lines compared with that in TP309 when both were inoculated with *M. oryzae*. Reverse transcription-quantitative PCR was performed using the *M. oryzae β-Tubulin* gene as internal control. (e) The invasive growth decreased in the *MoATI1-RNAi* lines. Infection hyphae types of *M. oryzae* B157 were counted at 40 h post-inoculation. Bar = 10 μm. Number of panicles (f), grain number per panicle (g) and 1000-grain weight (h) of the wild-type TP309 and *MoATI1-RNAi* lines displayed no difference. $T_2$ transgenic plants from two independent transgenic lines were used for all phenotypic analyses. The data represent mean ± *SD*. The asterisks represent significant differences analysed with Student's *t* test at $p < 0.001$.

et al., 2023; Quinsay et al., 2010; Shu et al., 2021; Wei et al., 2017). Taken together, MoAti1 participates in mitophagy by facilitating recruitment of MoAtg8 in *M. oryzae*, and may be the first mitophagy receptor identified in *M. oryzae*.

*M. oryzae* is a hemibiotrophic filamentous ascomycete (Dean et al., 2012). It initially acquires nutrients from living host cells and then switches to a necrotrophic phase, to acquire nutrients from dead tissues. During the shifts in fungal lifestyles, the invasive hyphae of *M. oryzae* are required to adapt to and overcome nutrient-stress conditions prior to switching to the necrotrophic phase. In a previous study, it was shown that mitophagy plays a critical role in the invasive growth of *M. oryzae* in response to energy demands and nutrient homeostasis (Kou et al., 2019). Disruption of the mitophagy-assisted gene *MoATG24* and several mitophagy-related genes, such as *MoDNM1*, *MoFIS1*, *MoMDV1* and *MoAUH1*, resulted in the similar phenotypes including reduced invasive hyphal growth and blast lesion formation (He et al., 2013; Xiao et al., 2021; Zhong et al., 2016), suggesting that mitophagy is required for the spread of invasive hyphae in *M. oryzae*. Consistent with these findings, disruption of *MoATI1* results in defects of invasive growth and pathogenicity. Further microscopic observation revealed that the reduced invasive hyphal growth in Δ*Moati1* may be attributed to abnormal mitophagy in the invasive hyphae, indicating that MoAti1-mediated mitophagy in *M. oryzae* is required for the establishment of blast disease. The precise regulatory mechanisms underlying MoAti1-mediated mitophagy during infection would certainly require further investigation in future research.

HIGS of fungal pathogenicity genes has been developed as a durable strategy to control fungal diseases. HIGS of pathogenic fungus-specific genes in host plants such as rice, wheat, barley and banana reduced fungal development and virulence (Dou et al., 2020; Nowara et al., 2010; Wang et al., 2020; Wang & Dean, 2022). In the rice–*M. oryzae* pathosystem, pathogenicity genes such as *MoMAC1*, *MoPMK1*, *MoMAGB*, *MoCRZ1*, *MoAP1* and *CYP51* have been confirmed to be efficient targets for HIGS to enhance blast resistance in rice (Wang & Dean, 2022; Zhu et al., 2017). These targets are

primarily required for the early infection process, including appressoria development and penetration. Here, we found that MoAti1 is required for invasive growth following penetration in *M. oryzae*. Notably, the absence of an MoAti1 homologue in rice and human minimizes the risk of off-target effects via HIGS. Silencing of the *MoATI1* gene through HIGS effectively suppressed the invasive growth of *M. oryzae* in the *MoATI1*-RNAi transgenic plants and did not affect agronomic traits, highlighting the potential of *MoATI1* as a valuable target for future strategies in rice blast control.

In summary, this study proposes a working model of MoAti1 regulating mitophagy of *M. oryzae* (Figure 8). Upon nitrogen starvation or when adapting to and overcoming nutrient stress prior to switching to the necrotrophic phase, MoAti1 facilitates the recruitment of MoAtg8, leading to the selective degradation of excessive or damaged mitochondria through mitophagy. Importantly, MoAti1-mediated mitophagy contributes to the invasive growth in *M. oryzae*, resulting in the establishment of blast disease in rice. Based on these results, it is further suggested that MoAti1-mediated mitophagy could serve as a promising target for chemicals or HIGS approaches with the aim of effectively controlling rice blast.

## 4 | EXPERIMENTAL PROCEDURES

### 4.1 | Fungal strains and culture media

The *M. oryzae* strains *Mito-GFP*, Δ*Moatg8/Mito-GFP*, *GFP-SRL and MoPEX14-GFP* have been described in our previous reports (Deng et al., 2013; He et al., 2013; Kou et al., 2019; Ramos-Pamplona & Naqvi, 2006). The strains used in this study are summarized in Table S3.

For growth and conidia collection, *M. oryzae* strains were grown on prune agar (PA; yeast extract 1 g/L, lactose 2.5 g/L, sucrose 2.5 g/L, prune juice 40 mL/L, agar 20 g/L, pH 6.5) at 28°C in the dark for 2 days, followed by growth under continuous light for 5 days. For a collection of mycelia, strains were cultured on complete medium (CM) for 2 days. Mutants generated by *Agrobacterium tumefaciens*-mediated transformation (ATMT) were selected on basal medium (BM; yeast nitrogen base 1.6 g/L, asparagine 2 g/L, $NH_4NO_3$ 1 g/L, glucose 10 g/L, agar 20 g/L, pH 6.0) with hygromycin (250 μg/mL), chlorimuron-ethyl (50 μg/mL), ammonium glufosinate (50 μg/mL) or G418 (400 μg/mL). The values of phenotype were calculated from three independent replicates and represented as the mean ± *SD*.

### 4.2 | Plasmids and strains construction

The *MoATI1* gene (*MGG_00505*) deletion mutant was generated using the standard one-step gene replacement strategy. Briefly, about 1 kb of 5′ untranslated region (UTR) and 3′ UTR were PCR amplified and ligated sequentially to flank the *sulfonylurea-resistance* gene cassette in pFGL820 (Addgene) (Figure S4). The primers used to amplify the 5′ and 3′ UTR of *MoATI1* gene are listed in Table S4. The final plasmid construct was confirmed by sequencing and subsequently introduced into the *Mito-GFP* strain by ATMT to replace *MoATI1* gene (Yang & Naqvi, 2014). The resultant transformants were ascertained by locus-specific PCR and Southern blot analyses (Figure S4). The *mCherry-MoATG8* construct was generated as previously described and transformed into the *Mito-GFP* and *M. oryzae* B157 to obtain the *mCherry-MoATG8/Mito-GFP* and *mCherry-MoATG8* strains (He et al., 2018). Δ*Moati1/GFP-MoATG8*, Δ*Moati1/mCherry-MoATG8/Mito-GFP*, Δ*Moati1/GFP-SRL* and Δ*Moati1/MoPEX14-GFP*

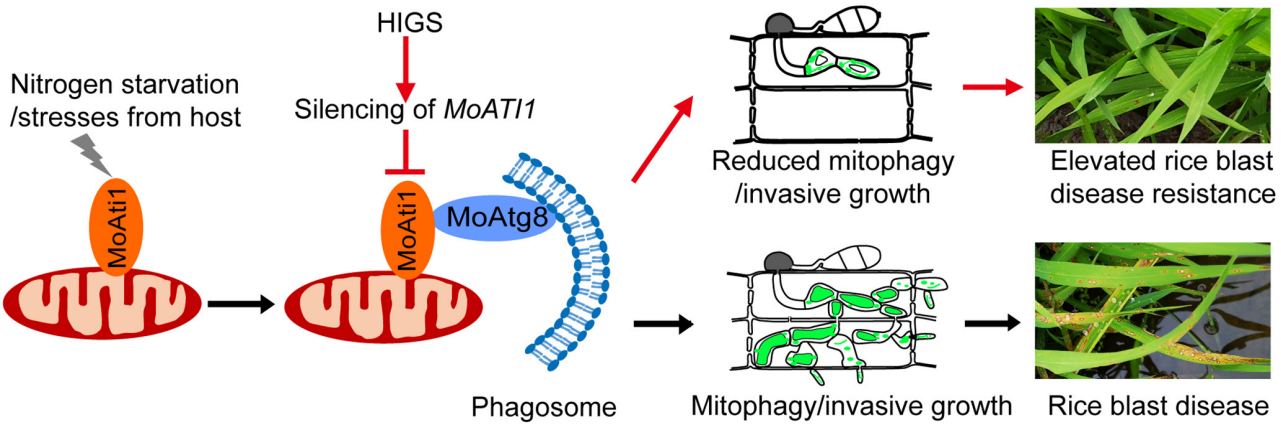


**FIGURE 8** Schematic model depicts that *MoATI1* regulates mitophagy to facilitate invasive growth in rice and host-induced gene silencing of *MoATI1* enhances resistance to rice blast. MoAti1 is primarily located in the peripheral mitochondrial outer membrane in *Magnaporthe oryzae*. Under conditions such as nitrogen starvation or nutrient stress during invasive growth, MoAti1 recruits the core autophagy-related protein MoAtg8 to the mitochondria, initiating the process of mitophagy in *M. oryzae*. This, in turn, promotes invasive growth and ultimately leads to the development of blast lesions. In transgenic plants expressing the *MoATI1* RNAi cassette, the invasive colonization of *M. oryzae* is reduced. In the diagram, the green dots or lines represent Mito-GFP (a mitochondrial marker) and the degraded Mito-GFP enters the vacuoles.

strains were generated by disruption of *MoATI1* in the *GFP-MoATG8*, *mCherry-MoATG8/Mito-GFP*, *GFP-SRL* and *MoPEX14-GFP* with a similar method. For complementation analysis, the full-length genomic copy with the promoter of *MoATI1* was amplified and inserted into pFGL822 (Addgene), then introduced into the Δ*Moati1/Mito-GFP* strain by ATMT.

The *MoATI1-mCherry* construct was generated by cloning the *MoATI1* fragment amplified with primers MoATI1-icF/MoATI1-mcR into pFGL822-*mCherry*. The resulting pFGL822-*MoATI1-mCherry* construct was confirmed by sequencing and transformed into the *Mito-GFP*, Δ*Moati1/Mito-GFP* or Δ*Moati1/GFP-MoATG8* via ATMT to produce *MoATI1-mCherry/Mito-GFP*, *MoATI1-mCherry/Mito-GFP/*Δ*Moati1* and *MoATI1-mCherry/*Δ*Moati1/GFP-MoATG8*, respectively. Then, the *MoATG8* gene was deleted in the resultant *MoATI1-mCherry/*Δ*Moati1/Mito-GFP* strain to obtain the Δ*Moatg8/*Δ*Moati1/MoATI1-mCherry/Mito-GFP* strain. Similarly, $MoATI1^{1,4,6AIM}$*-mCherry* fusion constructs were generated by cloning into pFGL823 and transformed into the Δ*Moati1/GFP-MoATG8* strain to produce the $MoATI1^{1,4,6AIM}$*-mCherry/*Δ*Moati1/GFP-MoATG8* strain, which was used for co-localization and Co-IP assays. The mutated gene $MoATI1^{1,4,6AIM}$ driven by its native promoter was cloned into pFGL823 and transformed into the Δ*Moati1/mCherry-MoATG8/Mito-GFP* strain to obtain $MoATI1^{1,4,6AIM}$*/*Δ*Moati1/mCherry-MoATG8/Mito-GFP*. Primers used in the construction of fluorescent vectors are listed in Table S4.

## 4.3 | Mitophagy, macroautophagy and pexophagy analysis

For observation of mitophagy in mycelia, strains expressing Mito-GFP were first cultured in CM for 2 days and then transferred to BM with glycerol for 30 h. Mycelia were treated with MM−N medium (minimal medium yeast nitrogen base without amino acids and ammonium sulphate 1.7 g/L, and glucose 20 g/L) containing 1 mM PMSF for 12 h before microscopic observation (He et al., 2013). For observation of macroautophagy, strains expressing *GFP-MoATG8* were cultured in CM for 2 days and transferred to SD−N (synthetic dropout medium without nitrogen) medium containing 1 mM PMSF. For observation of pexophagy, strains expressing *GFP-SRL* and *MoPEX14-GFP* were cultured in CM for 2 days and transferred to MM−N for 12 h. For vacuolar staining, the mycelia were stained with 10 μM CellTracker Blue CMAC dye (7-amino-4-chloromethyl coumarin; Molecular Probes) for 30 min at room temperature, and then washed with deionized water prior to microscopic observation. For biochemical assays, mycelial samples were treated as described above to induce mitophagy, macroautophagy or pexophagy and harvested for detection of Mito-GFP, GFP-MoAtg8 or MoPex14-GFP by immunoblot analysis.

To observe mitophagy in the invasive hyphae in *M. oryzae*, conidial suspensions ($10^5$/mL) harvested from 7-day-old culture plates were inoculated on the excised rice sheaths. Fluorescence of Mito-GFP in the invasive hyphae was monitored at 60 hpi.

## 4.4 | Fluorescence microscopy

Live cell epifluorescence microscopy was performed with an LSM 700 inverted confocal microscope (Carl Zeiss) equipped with a plan-apochromat 63 (NA = 1.40) oil immersion lens. CMAC, EGFP and mCherry excitation were performed at 405 nm (emission 430–470 nm), 488 nm (emission 505–530 nm) and 555 nm (emission 600–625 nm), respectively. The mycelia and in planta invasive hyphae observation and image processing with ImageJ software (http://rsb.info.nih.gov/) were performed as described (He et al., 2013; Kou et al., 2019). In order to prepare the figures, the images were laid out in Adobe Illustrator CS6.

## 4.5 | Y2H analysis

Y2H assays were performed with the DUALmembrane starter kit SUC system (Dualsystems Biotech) according to the manufacturer's instruction. The *MoATG8* open reading frame (ORF) was cloned into the pPR3-N vector as the prey vector. The *MoATI1* ORF and *AIM/LIR* mutants were amplified and ligated to pBT3-SUC as bait vectors. The resultant paired bait and prey vectors were transformed into yeast cells of the NMY51 strain. Yeast cells grown on the SD−Leu/Trp medium were assayed for growth on the SD−Trp/Leu/His/Ade medium. The paired plasmids of pTSUC2-APP and NubG-Fe65 were used as the positive control, while pTSUC2-APP and pPR3-N were served as the negative control.

## 4.6 | Immunoblot assay

To detect GFP and mCherry-tagged proteins, total protein was extracted with lysis buffer (50 mM Tris−HCl pH 7.4, 150 mM NaCl, 1 mM EDTA, 1% Triton 100, and 1 × protein inhibitor). To detect Porin protein levels, mycelia were ground and boiled with 10% SDS for 10 min before centrifugation at 12,000 *g* for 20 min. The resulting protein solution was separated by 8%–15% SDS-PAGE and transferred to PVDF membrane, subsequently detected by immunoblotting with anti-GFP (Huabio, ET1607-31), anti-mCherry (Invitrogen), anti-GAPDH (R1208-3) or anti-Porin antibodies (GenScript). The GAPDH protein served as a loading control. Horseradish peroxidase-conjugated secondary antibodies and an ECL kit (Bio-Rad) were used to detect the chemiluminescent signals. The relative intensities of the blots were quantified by ImageJ software.

## 4.7 | Co-IP assays

For the Co-IP assay of verifying the interaction between GFP-MoAtg8 and MoAti1-mCherry or AIM/LIR-mutated MoAti1-mCherry, total proteins were extracted as input and incubated with 25 μL of GFP-Trap magnetic beads (ChromoTek) according to the

manufacturer's instructions. The input and eluted protein solutions were separated on 10% SDS-PAGE and immunoblotted with anti-mCherry or anti-GFP antibodies.

### 4.8 | GST pull-down

For the pull-down assay, the coding sequence of MoAti1 was cloned into the pET28a vector to express the fusion protein His-MoAti1. The GST-MoAtg8 vector was kindly provided by Dr Xueming Zhu (Zhu et al., 2023). Both constructions were expressed in *E. coli* BL21 (DE3). The GST pull-down assay was performed with a GST 4FF sefinose resin kit (Sangon Biotech). Briefly, the supernatant containing GST-MoAtg8 or GST after ultrasonic disruption and centrifugation was incubated with 25 μL magnetic glutathione beads (Sigma) and the supernatant containing the fusion protein His-MoAti1 overnight at 4°C. Beads were washed three times with GST binding/washing buffer and eluted with elution buffer. Input and output protein samples were separated by SDS-PAGE and detected with immunoblot analysis using anti-GST (Huabio) and anti-His (Huabio) antibodies.

### 4.9 | BiFC assays

The cDNA fragment encoding MoAti1 was amplified and ligated into the pKD2-YFPN vector to obtain the resultant vector MoAti1-YFPN. The YFPC-MoAtg8 vector was kindly provided by Dr Xueming Zhu (Zhu et al., 2023). Pairs of MoAti1-YFPN and YFPC-MoAtg8 were co-transformed into *M. oryzae* B157 by the ATMT method. Pairs of MoAti1-YFPN and YFPC, YFPN and YFPC-MoAtg8, YFPN and YFPC were transformed with a similar strategy and used as negative controls. The fluorescence signal of the resultant transformants was observed with a Zeiss LSM 700 microscope.

### 4.10 | Infection assays

For the rice seedling infection assay, $10^6$/mL conidial suspension was sprayed on the 21-day-old rice seedlings (cv. CO39) and incubated in a growth chamber (16 h light/day, 22°C and 90% humidity). Blast disease symptoms and relative fungal biomass were assessed and recorded by scanning the inoculated leaves at 7 dpi (days post-inoculation) as previously described (Qiu et al., 2022). The rice seedling infection assays were performed with at least three replicates.

For the rice sheath infection assay, 21-day-old rice seedlings (CO39) were selected for sheath preparation. A conidial suspension ($5 \times 10^4$/mL) was inoculated onto the rice sheath and incubated under the high humidity conditions with a photoperiod of 16 h:8 h light:dark cycle at 22°C. The inoculated rice sheath was trimmed manually and observed by using an Olympus BX53 wide-field microscope or a laser-scanning confocal microscope at selected time points.

### 4.11 | RT-qPCR assay

Total RNA was extracted from mycelia cultured in CM for 2 days and *M. oryzae*-inoculated rice leaves using TRIzol (Invitrogen). The resulting total RNA was reverse transcribed, and qPCRs were carried out with SYBR Green according to protocols provided by the manufacturer (TaKaRa). The constitutively expressed *Tubulin* gene (*MGG_00604*) was used as an endogenous control to normalize the amount of cDNA templates. Primers used in the experiments are listed in Table S4.

### 4.12 | Isolation of mitochondria, sodium carbonate extraction and proteinase K treatment

Mycelia (0.1 g) of the strain expressing *MoATI1-GFP* and *MoTIM23-mCherry* were collected following culturing in CM with shaking for 2 days at 22°C and 150 rpm. Isolation of mitochondria was performed with a cell mitochondrial isolation kit (Beyotime). The resultant mitochondria were incubated in 100 μL of cold 0.1 M $Na_2CO_3$, pH 11 for 30 min on ice and then centrifuged for 30 min at 90,000 *g* at 4°C according to a previous report (Kim et al., 2015). The resultant supernatant and pellet were mixed with 500 μL of 12.5% trichloroacetic acid (TCA) solution for 30 min on ice and then centrifuged at 28,000 *g* for 15 min at 4°C. The pellets washed with acetone were dried at room temperature and incubated with 40 μL of 8 M urea and 2% SDS solution. The proteins MoAti1-GFP, MoTim23-mCherry and Porin were detected by the corresponding antibodies in an immunoblotting assay.

For proteinase K digestion, the strain expressing *MoATI1-GFP* and *MoCOX11-mCherry* was cultured in CM for 2 days at 28°C. The mycelia (1 g) were collected and ground with liquid nitrogen. The isolated mitochondria were dissolved with mito buffer (0.885 g/L sucrose, 7.45 mg/L KCl, 4.06 mg/L $MgCl_2.6H_2O$, 3.72 mg/L EDTA, 23.8 mg/L HEPES, pH 7.4) supplemented with a final concentration of 0.2, 0.8, 1, 5, 10, 50 and 100 μg/mL proteinase K for 20 min. The reaction solutions were stopped with 1 mM PMSF and boiled following adding 50 μL loading buffer. The protein amounts of MoAti1-GFP, MoCox11-mCherry, Porin and MoHsp60 were detected by the immunoblot assay. The relative protein levels of MoAti1-GFP, MoCox11-mCherry, Porin and MoHsp60 were evaluated using ImageJ software.

### 4.13 | Construction and agronomy traits measurement of transgenic rice

The *MoATI1* RNAi construct was generated and then inserted into the ds1301 vector as previously described (Chen et al., 2022).

Briefly, a sense DNA fragment containing 564-bp (position 401–964 nucleotides of the coding sequence) and the respective antisense sequence were inserted into the flanking region of the *WAXY* sequence. The sequenced construct was introduced into *A. tumefaciens* EHA105 by electroporation. ATMT of rice was performed by Wuhan BioRun Biosciences Co., Ltd. Transgenic plants were planted in the rice-growing season on the genetically modified experimental paddy fields of the China National Rice Research Institute, Hangzhou, China. The number of panicles, grain number per panicle, 1000-seed weight, plant height, grain length and grain width were determined as previously described (Li, Wei, et al., 2022).

## ACKNOWLEDGEMENTS

This research was supported by grants from the National Natural Science Foundation of China (32100161 to J.Q., 32000103 to Y.K.), National Key Research and Development Program (2022YFD1401500 and 2023YFD1400200), Key R&D project of China National Rice Research Institute, grand number (CNRRI-2020-04) and Key Projects of Zhejiang Provincial Natural Science Foundation (LZ23C130002 to J.Q.). This project was also supported by the Chinese Academy of Agricultural Sciences under the 'Elite Youth' Program and the Agricultural Sciences and Technologies Innovation Program. We thank Professor Wangzhong Ge, Chao Tong, Yizhen Deng, Xueming Zhu and Rice–Pathogen Interaction group at China National Rice Research Institute for providing vector resources, useful discussion and suggestions.

## CONFLICT OF INTEREST STATEMENT

The authors declare that there are no conflicts of interest related to this article.

## DATA AVAILABILITY STATEMENT

All data generated or analysed during the present study can be found within the manuscript and the supplemental files. The *M. oryzae* genes from this article can be found in the GenBank database at https://www.ncbi.nlm.nih.gov/genbank/ under the following accession numbers: *MoATI1* (*MGG_00505*), *MoATG8* (*MGG_01062*), *MoPEX14* (*MGG_01028*), *MoCOX11* (MGG_11431), *MoPORIN* (MGG_00968) and *MoTIM23* (MGG_08885).

## ORCID

*Chaoxi Luo* https://orcid.org/0000-0002-9385-9898
*Naweed I. Naqvi* https://orcid.org/0000-0002-3619-4906
*Yanjun Kou* https://orcid.org/0000-0003-4189-0962

## REFERENCES

Besingi, R.N. & Clark, P.L. (2015) Extracellular protease digestion to evaluate membrane protein cell surface localization. *Nature Protocols*, 10, 2074–2080.

Bhujabal, Z., Birgisdottir, Å., B., Sjøttem, E., Brenne, H.B., Øvervatn, A. et al. (2017) FKBP8 recruits LC3A to mediate Parkin-independent mitophagy. *EMBO Reports*, 18, 947–961.

Cai, Q., Qiao, L., Wang, M., He, B., Lin, F.M., Palmquist, J. et al. (2018) Plants send small RNAs in extracellular vesicles to fungal pathogen to silence virulence genes. *Science*, 360, 1126–1129.

Camougrand, N., Grelaud-Coq, A., Marza, E., Priault, M., Bessoule, J.J. & Manon, S. (2003) The product of the *UTH1* gene, required for Bax-induced cell death in yeast, is involved in the response to rapamycin. *Molecular Microbiology*, 47, 495–506.

Camougrand, N.M., Mouassite, M., Velours, G.M. & Guérin, M.G. (2000) The "SUN" family: UTH1, an ageing gene, is also involved in the regulation of mitochondria biogenesis in *Saccharomyces cerevisiae*. *Archives of Biochemistry and Biophysics*, 375, 154–160.

Chen, X., Pei, Z., Liu, H., Huang, J., Chen, X., Luo, C. et al. (2022) Host-induced gene silencing of fungal-specific genes of *Ustilaginoidea virens* confers effective resistance to rice false smut. *Plant Biotechnology Journal*, 20, 253–255.

Dean, R., Van Kan, J.A.L., Pretorius, Z.A., Hammond-Kosack, K.E., Di Pietro, A., Spanu, P.D. et al. (2012) The top 10 fungal pathogens in molecular plant pathology. *Molecular Plant Pathology*, 13, 414–430.

Deng, Y., Qu, Z. & Naqvi, N.I. (2013) The role of Snx41-based pexophagy in *Magnaporthe* development. *PLoS One*, 8, e79128.

Dou, T., Shao, X., Hu, C., Liu, S., Sheng, O., Bi, F. et al. (2020) Host-induced gene silencing of Foc TR4 ERG6/11 genes exhibits superior resistance to *Fusarium* wilt of banana. *Plant Biotechnology Journal*, 18, 11–13.

Feng, Y., He, D., Yao, Z. & Klionsky, D.J. (2014) The machinery of macroautophagy. *Cell Research*, 24, 24–41.

Fracchiolla, D., Sawa-Makarska, J. & Martens, S. (2017) Beyond Atg8 binding: the role of AIM/LIR motifs in autophagy. *Autophagy*, 13, 978–979.

Friedman, J.R. & Nunnari, J. (2014) Mitochondrial form and function. *Nature*, 505, 335–343.

Fukuda, T., Ebi, Y., Saigusa, T., Furukawa, K., Yamashita, S.I., Inoue, K. et al. (2020) Atg43 tethers isolation membranes to mitochondria to promote starvation-induced mitophagy in fission yeast. *eLife*, 9, e61245.

He, M., Xu, Y., Chen, J., Luo, Y., Lv, Y., Su, J. et al. (2018) MoSnt2-dependent deacetylation of histone H3 mediates MoTor-dependent autophagy and plant infection by the rice blast fungus *Magnaporthe oryzae*. *Autophagy*, 14, 1543–1561.

He, Y., Deng, Y.Z. & Naqvi, N.I. (2013) Atg24-assisted mitophagy in the foot cells is necessary for proper asexual differentiation in *Magnaporthe oryzae*. *Autophagy*, 9, 1818–1827.

Jacomin, A.C., Samavedam, S., Promponas, V. & Nezis, I.P. (2016) iLIR database: a web resource for LIR motif-containing proteins in eukaryotes. *Autophagy*, 12, 1945–1953.

Khan, I.A., Ning, G., Liu, X., Feng, X., Lin, F. & Lu, J. (2015) Mitochondrial fission protein MoFis1 mediates conidiation and is required for full virulence of the rice blast fungus *Magnaporthe oryzae*. *Microbiological Research*, 178, 51–58.

Kim, H., Botelho, S.C., Park, K. & Kim, H. (2015) Use of carbonate extraction in analyzing moderately hydrophobic transmembrane proteins in the mitochondrial inner membrane. *Protein Science*, 24, 2063–2069.

Kissova, I., Deffieu, M., Manon, S. & Camougrand, N. (2004) Uth1p is involved in the autophagic degradation of mitochondria. *The Journal of Biological Chemistry*, 279, 39068–39074.

Klionsky, D.J., Abdel-Aziz, A.K., Abdelfatah, S., Abdellatif, M., Abdoli, A., Abel, S. et al. (2021) Guidelines for the use and interpretation of assays for monitoring autophagy (4th edition)(1). *Autophagy*, 17, 1–382.

Kou, Y., He, Y., Qiu, J., Shu, Y., Yang, F., Deng, Y. et al. (2019) Mitochondrial dynamics and mitophagy are necessary for proper invasive growth in rice blast. *Molecular Plant Pathology*, 20, 1147–1162.

Li, C., Duckney, P., Zhang, T., Fu, Y., Li, X., Kroon, J. et al. (2022) TraB family proteins are components of ER-mitochondrial contact sites and regulate ER-mitochondrial interactions and mitophagy. *Nature Communications*, 13, 5658.

Li, L., Zhu, X.M., Liu, X.H. & Lin, F.C. (2021) Methods to study autophagocytosis in *Magnaporthe oryzae*. *Methods in Molecular Biology*, 2356, 173–185.

Li, Z., Wei, X., Tong, X., Zhao, J., Liu, X., Wang, H. et al. (2022) The OsNAC23-Tre6P-SnRK1a feed-forward loop regulates sugar homeostasis and grain yield in rice. *Molecular Plant*, 15, 706–722.

Liu, L., Feng, D., Chen, G., Chen, M., Zheng, Q., Song, P. et al. (2012) Mitochondrial outer-membrane protein FUNDC1 mediates hypoxia-induced mitophagy in mammalian cells. *Nature Cell Biology*, 14, 177–185.

Liu, L., Sakakibara, K., Chen, Q. & Okamoto, K. (2014) Receptor-mediated mitophagy in yeast and mammalian systems. *Cell Research*, 24, 787–795.

Liu, W., Liu, Z., Mo, Z., Guo, S., Liu, Y. & Xie, Q. (2021) ATG8-interacting motif:evolution and function in selective autophagy of targeting biological processes. *Frontiers in Plant Science*, 12, 783881.

Mehta, M.M., Weinberg, S.E. & Chandel, N.S. (2017) Mitochondrial control of immunity: beyond ATP. *Nature Reviews Immunology*, 17, 608–620.

Meyer, L.M., Koschade, S.E., Vischedyk, J.B., Thoelken, M., Gubas, A., Wegner, M. et al. (2023) Deciphering the mitophagy receptor network identifies a crucial role for OPTN (optineurin) in acute myeloid leukemia. *Autophagy*, 19, 2982–2996.

Mouassite, M., Camougrand, N., Schwob, E., Demaison, G., Laclau, M. & Guérin, M. (2000) The 'SUN' family: yeast SUN4/SCW3 is involved in cell septation. *Yeast*, 16, 905–919.

Mouassite, M., Guérin, M.G. & Camougrand, N.M. (2000) The SUN family of *Saccharomyces cerevisiae*: the double knock-out of *UTH1* and *SIM1* promotes defects in nucleus migration and increased drug sensitivity. *FEMS Microbiology Letters*, 182, 137–141.

Murakawa, T., Yamaguchi, O., Hashimoto, A., Hikoso, S., Takeda, T., Oka, T. et al. (2015) Bcl-2-like protein 13 is a mammalian Atg32 homologue that mediates mitophagy and mitochondrial fragmentation. *Nature Communications*, 6, 7527.

Nagi, M., Tanabe, K., Nakayama, H., Ueno, K., Yamagoe, S., Umeyama, T. et al. (2016) Iron-depletion promotes mitophagy to maintain mitochondrial integrity in pathogenic yeast *Candida glabrata*. *Autophagy*, 12, 1259–1271.

Nakatogawa, H., Ichimura, Y. & Ohsumi, Y. (2007) Atg8, a ubiquitin-like protein required for autophagosome formation, mediates membrane tethering and hemifusion. *Cell*, 130, 165–178.

Ng, M.Y.W., Wai, T. & Simonsen, A. (2021) Quality control of the mitochondrion. *Developmental Cell*, 56, 881–905.

Novak, I., Kirkin, V., McEwan, D.G., Zhang, J., Wild, P., Rozenknop, A. et al. (2010) Nix is a selective autophagy receptor for mitochondrial clearance. *EMBO Reports*, 11, 45–51.

Nowara, D., Gay, A., Lacomme, C., Shaw, J., Ridout, C., Douchkov, D. et al. (2010) HIGS: host-induced gene silencing in the obligate biotrophic fungal pathogen *Blumeria graminis*. *The Plant Cell*, 22, 3130–3141.

Okamoto, K., Kondo-Okamoto, N. & Ohsumi, Y. (2009) Mitochondria-anchored receptor Atg32 mediates degradation of mitochondria via selective autophagy. *Developmental Cell*, 17, 87–97.

Onishi, M., Yamano, K., Sato, M., Matsuda, N. & Okamoto, K. (2021) Molecular mechanisms and physiological functions of mitophagy. *The EMBO Journal*, 40, e104705.

Palikaras, K., Lionaki, E. & Tavernarakis, N. (2018) Mechanisms of mitophagy in cellular homeostasis, physiology and pathology. *Nature Cell Biology*, 20, 1013–1022.

Panigrahi, D.P., Praharaj, P.P., Behera, B.P., Patra, S., Patil, S., Patro, B.S. et al. (2023) The inner mitochondrial membrane fission protein MTP18 serves as a mitophagy receptor to prevent apoptosis in oral cancer. *Journal of Cell Science*, 136, jcs259986.

Patkar, R.N., Ramos-Pamplona, M., Gupta, A.P., Fan, Y. & Naqvi, N.I. (2012) Mitochondrial beta-oxidation regulates organellar integrity and is necessary for conidial germination and invasive growth in *Magnaporthe oryzae*. *Molecular Microbiology*, 86, 1345–1363.

Qiu, J., Xie, J., Chen, Y., Shen, Z., Shi, H., Naqvi, N.I. et al. (2022) Warm temperature compromises JA-regulated basal resistance to enhance *Magnaporthe oryzae* infection in rice. *Molecular Plant*, 15, 723–739.

Quinsay, M.N., Thomas, R.L., Lee, Y. & Gustafsson, A.B. (2010) Bnip3-mediated mitochondrial autophagy is independent of the mitochondrial permeability transition pore. *Autophagy*, 6, 855–862.

Ramos-Pamplona, M. & Naqvi, N.I. (2006) Host invasion during rice-blast disease requires carnitine-dependent transport of peroxisomal acetyl-CoA. *Molecular Microbiology*, 61, 61–75.

Shu, L., Hu, C., Xu, M., Yu, J., He, H., Lin, J. et al. (2021) ATAD3B is a mitophagy receptor mediating clearance of oxidative stress-induced damaged mitochondrial DNA. *The EMBO Journal*, 40, e106283.

Valent, B. (2021) The impact of blast disease: past, present, and future. In: Jacob, S. (Ed.) *Magnaporthe oryzae: methods and protocols*. New York, NY: Springer US, pp. 1–18.

Velours, G., Boucheron, C., Manon, S. & Camougrand, N. (2002) Dual cell wall/mitochondria localization of the 'SUN' family proteins. *FEMS Microbiology Letters*, 207, 165–172.

Veneault-Fourrey, C., Barooah, M., Egan, M., Wakley, G. & Talbot, N.J. (2006) Autophagic fungal cell death is necessary for infection by the rice blast fungus. *Science*, 312, 580–583.

Wang, M. & Dean, R.A. (2022) Host induced gene silencing of *Magnaporthe oryzae* by targeting pathogenicity and development genes to control rice blast disease. *Frontiers in Plant Science*, 13, 959641.

Wang, M., Wu, L., Mei, Y., Zhao, Y., Ma, Z., Zhang, X. et al. (2020) Host-induced gene silencing of multiple genes of *Fusarium graminearum* enhances resistance to *Fusarium* head blight in wheat. *Plant Biotechnology Journal*, 18, 2373–2375.

Wei, Y., Chiang, W.C., Sumpter, R., Jr., Mishra, P. & Levine, B. (2017) Prohibitin 2 is an inner mitochondrial membrane mitophagy receptor. *Cell*, 168, 224–238.e10.

Welter, E., Montino, M., Reinhold, R., Schlotterhose, P., Krick, R., Dudek, J. et al. (2013) Uth1 is a mitochondrial inner membrane protein dispensable for post-log-phase and rapamycin-induced mitophagy. *The FEBS Journal*, 280, 4970–4982.

Xiao, Y., Liu, L., Zhang, T., Zhou, R., Ren, Y., Li, X. et al. (2021) Transcription factor MoMsn2 targets the putative 3-methylglutaconyl-CoA hydratase-encoding gene *MoAUH1* to govern infectious growth via mitochondrial fusion/fission balance in *Magnaporthe oryzae*. *Environmental Microbiology*, 23, 774–790.

Xie, Z., Nair, U. & Klionsky, D.J. (2008) Atg8 controls phagophore expansion during autophagosome formation. *Molecular Biology of the Cell*, 19, 3290–3298.

Yan, X. & Talbot, N.J. (2016) Investigating the cell biology of plant infection by the rice blast fungus *Magnaporthe oryzae*. *Current Opinion in Microbiology*, 34, 147–153.

Yang, F. & Naqvi, N.I. (2014) Sulfonylurea resistance reconstitution as a novel strategy for *ILV2*-specific integration in *Magnaporthe oryzae*. *Fungal Genetics and Biology*, 68, 71–76.

Youle, R.J. & Narendra, D.P. (2011) Mechanisms of mitophagy. *Nature Reviews Molecular Cell Biology*, 12, 9–14.

Zhong, K., Li, X., Le, X., Kong, X., Zhang, H., Zheng, X. et al. (2016) MoDnm1 dynamin mediating peroxisomal and mitochondrial fission in complex with MoFis1 and MoMdv1 is important for development of functional appressorium in *Magnaporthe oryzae*. *PLoS Pathogens*, 12, e1005823.

Zhou, C., Huang, Y., Shao, Y., May, J., Prou, D., Perier, C. et al. (2008) The kinase domain of mitochondrial PINK1 faces the cytoplasm. *Proceedings of the National Academy of Sciences of the United States of America*, 105, 12022–12027.

Zhu, L., Zhu, J., Liu, Z., Wang, Z., Zhou, C. & Wang, H. (2017) Host-induced gene silencing of rice blast fungus *Magnaporthe oryzae* pathogenicity genes mediated by the brome mosaic virus. *Genes*, 8, 241.

Zhu, X.M., Li, L., Bao, J.D., Wang, J.Y., Liang, S., Zhao, L.L. et al. (2023) MoVast2 combined with MoVast1 regulates lipid homeostasis and autophagy in *Magnaporthe oryzae*. *Autophagy*, 19, 2353–2371.

Zutphen, T., Veenhuis, M. & van der Klei, I.J. (2008) Pex14 is the sole component of the peroxisomal translocon that is required for pexophagy. *Autophagy*, 4, 63–66.

## SUPPORTING INFORMATION

Additional supporting information can be found online in the Supporting Information section at the end of this article.

**How to cite this article:** Shi, H., Meng, S., Qiu, J., Xie, S., Jiang, N., Luo, C. et al. (2024) MoAti1 mediates mitophagy by facilitating recruitment of MoAtg8 to promote invasive growth in *Magnaporthe oryzae*. *Molecular Plant Pathology*, 25, e13439. Available from: https://doi.org/10.1111/mpp.13439